IEEE Access
Multidisciplinary | Rapid Review | Open Access Journal

Received December 24, 2020, accepted January 13, 2021, date of publication January 20, 2021, date of current version January 29, 2021.

Digital Object Identifier 10.1109/ACCESS.2021.3053002

Trade-off Optimization Method for Infrared Imaging System Based on Modification of λF/d

KE LI, YING YUAN, CHAO ZHANG, HANG YUAN, AND XIAORUI WANG
School of Physics and Optoelectronic Engineering, Xidian University, Xi'an 710071, China

Corresponding authors: Ying Yuan (yuanying@xidian.edu.cn) and Xiaorui Wang (xrwang@mail.xidian.edu.cn)

This work was supported in part by the National Natural Science Foundation of China under Grant 62005204, Grant 62075176, and Grant 61775174; in part by the Equipment Advance Research Project of China under Grant 61400030202; and in part by the Natural Science Basic Research Plan in Shaanxi Province of China under Grant 2019JQ-071.

ABSTRACT The precise matching of the optical system and the detector has attracted more and more attention to satisfy requirements of future infrared (IR) imaging systems, both for miniaturization and long-distance detection. Considering the trade-off between the spatial resolution and the sensitivity, this paper proposes a general optimization method, which can optimize parameters of the IR imaging system automatically by modifying λF/d. Firstly, on the basis of the trade-off between the spatial transfer characteristics and the spatial sampling characteristics, we establish a more accurate minimum resolvable temperature difference (MRTD) model, and analyze the coupling relationship between the optical system and the detector under the optimum MRTD. Secondly, we analyze the relationship between parameters of the IR imaging system and MRTD model, and propose a trade-off optimization approach of the IR imaging system. Finally, this paper verifies the rationality of the optimization method by optimizing CA-295 system. The trade-off optimization method proposed in this paper can not only satisfy the design requirement, but also reduce the size, weight, power consumption and cost (SWaP$) of IR imaging systems.

INDEX TERMS Infrared imaging, spatial resolution, sensitivity, optimization methods, infrared detectors.

I. INTRODUCTION

Infrared (IR) imaging systems have become an essential tool in optical remote sensing [1], IR precise guidance [2], IR surveillance [3] and, deep-space exploration [4]. In order to reduce the size, weight, power consumption and cost (SWaP$) of IR imaging systems, it is necessary to reduce the optical system aperture and the detector size without reducing the comprehensive imaging performance [5]. The comprehensive performance of the IR imaging system is determined by the spatial resolution and the sensitivity [6], and λF/d determines the relationship between the optical system aperture and the detector size [7]–[9]. Therefore, in order to reduce the system SWaP$, it is necessary to consider the trade-off between the spatial resolution and the sensitivity, and propose an automatic optimization approach of IR imaging system based on the modification of λF/d.

Optimization method for the IR imaging system has been studied by many researchers. Bijl [10] used the contrast threshold of the TOD model as the objective function, and the sensor was analyzed and optimized to minimize the deviation between the output image and the recorded image by changing the value of the system parameter. Olson [11] took irradiance as the objective function, and the corresponding optimum detector size was optimized by changing the F-number under the conditions with fixed other system parameters. Holst [12] optimized the detector size by analyzing the field of view (FOV) and the number of pixels corresponding to the different detector sizes to design a high-count, small detector array. Liu [13] presented the analysis results about fill factor and stage number of TDI CMOS sensor. From the point of view of filling factor of detector, the design scheme of detector pixel size under optimum modulation transfer function (MTF) and signal-to-noise ratio (SNR) conditions is given. Abolghasemi and Abbasi-Moghadam [14] show an analysis method and corresponding analytical tools for design of the experimental imaging payload (IMPL) of a remote sensing satellite (SINA-1), they begin with top-level customer system performance requirements and constraints and derive the critical system and component parameters. The performance analysis is accomplished by calculating the imaging payload's signal-to-noise ratio (SNR), and imaging

The associate editor coordinating the review of this manuscript and approving it for publication was Shaoyong Zheng.

resolution. The above research work has contributed to the analysis and the optimization methods for the IR imaging system single-parameter, but there are few studies on the optimization method with considering the trade-off between the spatial resolution and the sensitivity.

In this paper, considering the above shortcomings, on the basis of the trade-off between the spatial resolution and the sensitivity, a general optimization method is proposed, which can inversely optimize the IR imaging system parameters. Firstly, regarding of the trade-off between the spatial transfer characteristics and the spatial sampling characteristics, we build a more accurate minimum resolvable temperature difference (MRTD) model, and propose an approach that can inversely modify λF/d. Then, by analyzing the changing trends of each IR system parameter on MRTD, this paper proposes a trade-off optimization method that can optimize system parameters simultaneously. Finally, by optimizing system parameters of CA-295, the rationality of the optimization method proposed in this paper is verified.

II. MODIFICATION OF λF/d BY MRTD MODEL

As a comprehensive performance index, MRTD not only represents the sensitivity of IR imaging system, but also characterizes the spatial resolution [15]. When the traditional MRTD model considers the influence of the spatial resolution, it only analyzes the signal spatial transfer characteristics, and ignores the signal aliasing caused by the spatial sampling characteristics. By considering the trade-off between the spatial transfer characteristics and the spatial sampling characteristics, this section firstly analyzes the relationship between λF/d and the spatial resolution model. Then, we build a more accurate MRTD model, and propose an approach to modify λF/d by MRTD, which can accurately analyze the coupling relationship between the optical system and the detector.

A. MODIFICATION OF λF/d BY SPATIAL RESOLUTION

MTF of an imaging system quantifies the ability of the system to resolve or transfer spatial frequencies [16], [17], [18]. In order to accurately describe the spatial resolution of the IR imaging system, we analyze the influence of the spatial transfer characteristics and the sampling characteristics on the spatial resolution quantitatively, and modify λF/d by the spatial resolution model.

1) SPATIAL TRANSFER CHARACTERISTICS

Typically, MTF before the detector sampling can represent the spatial transfer characteristics, and it can be determined through the multiplication of the theoretical MTF of each of the individual components (optical systems, detectors, etc.) [18]. For the IR imaging system MTF, there are two main considerations: the optical system MTF, and the detector MTF. The spatial transfer MTF of the IR imaging system is the multiplication of each of the individual MTF, and can be expressed as [18]:

$$MTF_{pre}(f) = MTF_o(f) \cdot MTF_d(f) \tag{1}$$

where $MTF_{pre}(f)$ is the spatial transfer MTF, f is the spatial frequency, $MTF_o(f)$, and $MTF_d(f)$ are MTF of the optical system, and the detector, respectively. The optical system MTF and the detector MTF are studied in previous work [19]–[21]. The focal length of the optical system is set to 1270mm, the detector size is 25μm, the integration time is 10ms, and the wavelength range is 3μm to 5μm. Fig. 1 shows the spatial transfer MTF curve.

On the basis of the Nyquist sampling theory, there is no signal aliasing when λF/d = 2.0, and the imaging system can reconstruct the digital signal into the analog image without distortion. However, according on Fig. 1, it can be seen that the spatial transfer MTF value at the Nyquist frequency is 0 when λF/d = 2.0, which leads to the low spatial resolution. In order to improve the spatial resolution, MTF value at the Nyquist frequency must be large enough, that is, λF/d < 2.0 is required. Meanwhile, the aliased signals are introduced when λF/d < 2.0. Therefore, it is necessary to comprehensively consider the spatial transfer MTF and aliasing MTF, and analyze the trade-off between the spatial transfer MTF and the signal aliasing.

2) SPATIAL SAMPLING CHARACTERISTICS

Signal aliasing is caused by the detector sampling, and the degree of the aliasing can be described by the spurious response MTF. The spurious response MTF of the first-order aliasing can be expressed as:

$$MTF_{sp}(f) = MTF_{pre}\left(f - f_{Nyquist}\right) \cdot MTF_{post}(f) \tag{2}$$

where $MTF_{sp}(f)$ is the spurious response MTF, $MTF_{post}(f)$ is MTF after the detector sampling.

Fig. 2 shows the spurious response MTF curve under different λF/d. According to Fig. 2, when λF/d value is 0.4, 0.8, 1.2, 1.6, and 2.0, the peak value of the spurious response MTF is 0.33, 0.21, 0.10, 0.03, and 0.01, respectively. That is, as λF/d value increases, the peak value of the spurious response MTF decreases. The in-band aliasing is zero when λF/d = 2.0, and out-of-band aliasing exists because of the non-ideal filter.

3) SPATIAL RESOLUTION MODEL BY TRADING-OFF SPATIAL TRANSFER CHARACTERISTICS AND SPATIAL SAMPLING CHARACTERISTICS

According to the above analysis, the spatial transfer characteristics and the spatial sampling characteristics affect the spatial resolution simultaneously. Therefore, the system spatial resolution needs to consider the trade-off between the spatial transfer MTF and the spurious response MTF. Fig. 3 shows the relationship between the spatial transfer MTF and the spurious response MTF at the Nyquist frequency.

On the basis of the design requirement, the spatial transfer MTF value at the Nyquist frequency should be greater than 0.2. At the same time, the spurious response method proposed by Shade believes that when the spurious response MTF value at the Nyquist frequency is smaller than 0.15 [22], signal

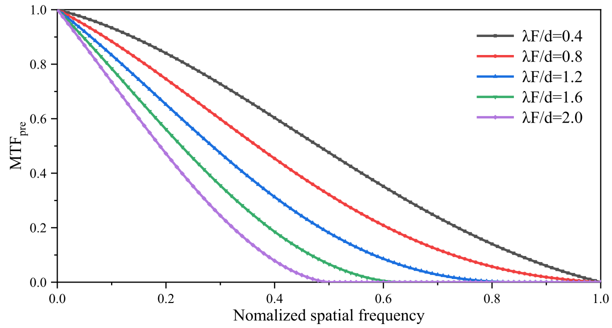

FIGURE 1. Spatial transfer MTF curves under different λF/d.

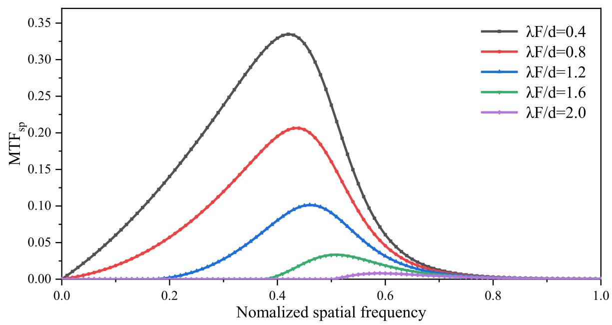

FIGURE 2. Spatial sampling MTF curves under different λF/d.

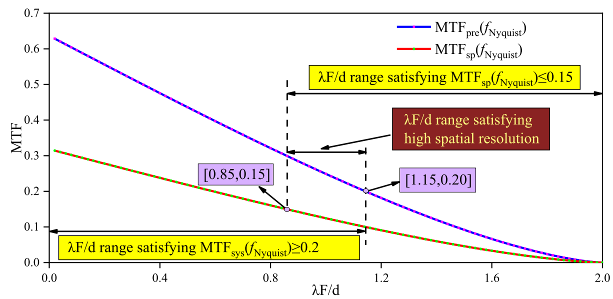

FIGURE 3. Trading-off between spatial transfer characteristics and spatial sampling characteristics.

aliasing does not affect the system image quality. It can be seen from Fig. 3 that when $0.85 < \lambda F/d < 1.15$, the system spatial resolution will not reduce the imaging quality.

In order to more accurately describe the coupling and matching relationship between the optical system and the detector under the optimum spatial resolution, we analyze the relationship between λF/d and the system MTF. The squeeze factor is calculated in previous work [22]. The system MTF after squeezing can be expressed as:

$$MTF_{sq}(f) = MTF_{pre}\left(\frac{f}{squeeze}\right) \tag{3}$$

where $MTF_{sq}(f)$ is the system MTF, *squeeze* is the squeeze factor.

Fig. 4 shows the curve of the spatial resolution model. Fig. 4(a) shows the system MTF curves under different λF/d, and Fig. 4(b) shows the system MTF value at the normalized spatial frequency of 0.5.

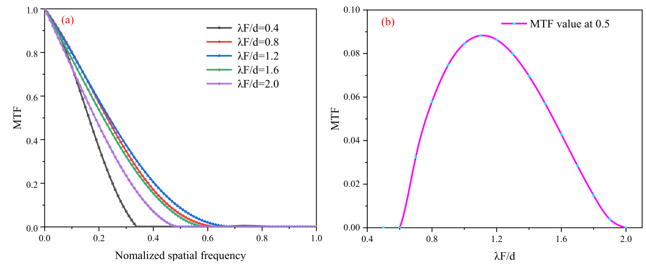

FIGURE 4. Spatial resolution model. (a) System MTF curves under different λF/d. (b) System MTF value at the normalized spatial frequency of 0.5.

Comparing Fig. 1 and Fig. 4(a), due to the influence of signal aliasing, the system cut-off frequency and the system MTF is reduced. The signal aliasing is the largest when $\lambda F/d = 0.4$, and the system MTF decreases the most. As λF/d increases, the signal aliasing decreases, and the system MTF decline trend becomes smaller and smaller. The signal aliasing has no effect on system MTF when $\lambda F/d = 2.0$.

Fig. 4(b) shows the curve of the system MTF value at the normalized spatial frequency of 0.5 when λF/d increases. Affected by the trade-off between spatial transfer MTF and spurious response MTF, the MTF value first increases and then decreases with the increase of λF/d. The spatial resolution is optimum when $\lambda F/d = 1.1$.

B. SENSITIVITY OF IR SYSTEM

In order to guarantee the sensitivity of the IR imaging system satisfying the requirement, this paper uses noise equivalent temperature difference (NETD) to represent the thermal sensitivity. NETD is a measure of noise phenomena, which is used to characterize the total noise information of the IR imaging system. NETD of the IR imaging system can be expressed as [8]:

$$NETD = \frac{4\sqrt{\Delta f_n}F^2}{\sqrt{A_d}\tau_o D^*_{\lambda_p}}\left[\frac{c_2}{\lambda_p T_B^2}\int_{\lambda_1}^{\lambda_2} M_\lambda(T_B)\,d\lambda\right]^{-1} \tag{4}$$

where Δf_n is the noise equivalent bandwidth of the IR imaging system, F is the F-number of the optical system, A_d is the pixel area of the detector, τ_0 is the optical system transmission, $D^*_{\lambda p}$ is the peak detectivity, c_2 is second radiation constant, $c_2 = 14388\ \mu m \cdot K$, λ_p is the peak wavelength, λ_1, λ_2 is the wavelength range, $M_\lambda(T_B)$ is the Planck formula, T_B is the background temperature. Fig. 5 shows NETD curve with the increasing of λF/d. It can be seen that NETD is monotonously increasing when λF/d increases.

C. MRTD MODEL BY TRADING-OFF SPATIAL RESOLUTION MODEL AND SENSITIVITY MODEL

Based on the above spatial resolution model and sensitivity model, when λF/d gradually increases, the spatial resolution first increases and then decreases, and the sensitivity always decreases. In order to modify λF/d by the system comprehensive performance, it is necessary to trade-off the influence of the spatial resolution and the sensitivity on MRTD, and establish a more accurate MRTD model. MRTD can be expressed

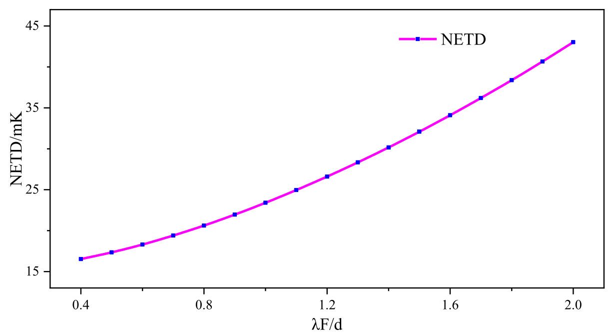

FIGURE 5. NETD curve.

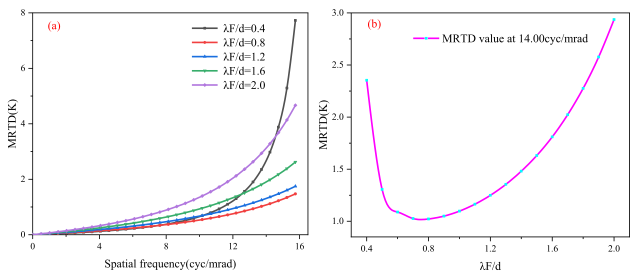

FIGURE 6. MRTD model. (a) MRTD curves under different λF/d. (b) MRTD value at the spatial frequency of 14.00cyc/mrad.

as:

$$MRTD\,(f) = \frac{\pi^2}{4\sqrt{14}} SNR_{TH} f \left(\frac{\alpha\beta}{t_{eye} f_p \Delta f_n \tau_d}\right)^{1/2} \cdot \frac{NETD}{MTF_{pre}\left(\frac{f}{squeeze}\right)} \tag{5}$$

where $\mathrm{SNR_{TH}}$ is the signal-to-noise ratio threshold, α and β are the instantaneous field of view (IFOV) of the detector in the horizontal and vertical direction, respectively, f_p is the frame rate, Δf_n is the noise equivalent bandwidth, t_{eye} is the eye integration time, τ_d is the detention time.

According to the above analysis, the spatial resolution is optimum when λF/d = 1.1, and the sensitivity is optimum when λF/d = 0.4. Considering the trade-off between the spatial resolution and the sensitivity, Fig. 6 shows the curve of MRTD model. Fig. 6(a) shows MRTD curves under different λF/d, and Fig. 6(b) shows MRTD value at the spatial frequency of 14.00cyc/mrad when λF/d value increases.

It can be seen from Fig. 6 that, as λF/d increases, because of the trade-off between the spatial resolution and the sensitivity, MRTD value at a specific spatial frequency first decreases and then increases. When λF/d = 0.8, MRTD value at the spatial frequency of 14.00cyc/mrad is the smallest, and the comprehensive system performance is the best.

Fig. 7 shows the simulation results at different λF/d. The physical size of the first-bar test target is set to 5.00m, the inherent temperature difference between the target and the background is 20K, the wavelength range is 3μm to 5μm, and the imaging distance is 7km.

On the basis of Fig. 7, the imaging quality of the system first improves and then decreases as λF/d increases. The sensitivity is high but the spatial resolution is low when

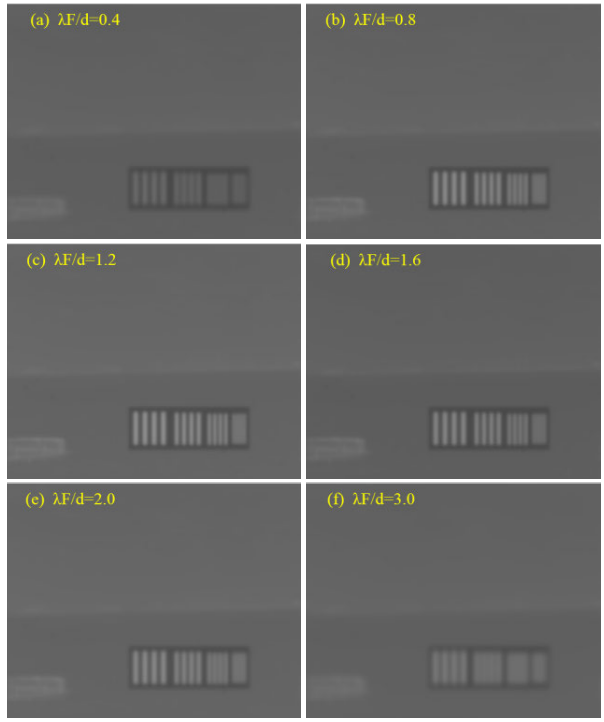

FIGURE 7. Simulation results under different λF/d.

λF/d = 0.4, which leads to the poor imaging quality. With the increase of λF/d, the sensitivity decreases but the spatial resolution increases. Considering the trade-off between the spatial resolution and the sensitivity, the imaging quality improves when λF/d = 1.2. As λF/d continues to increase, the spatial resolution and the sensitivity become worse simultaneously when λF/d = 3.0, which brings out the decrease of the imaging quality. Therefore, in the design process of the system, the selection of an appropriate λF/d plays an important role in the imaging quality. Based on the modification of λF/d by MRTD, this paper proposes an automatic optimization approach, which can optimize the optimum λF/d according to the different task requirement.

III. TRADE-OFF OPTIMIZATION APPROACH

In order to study the optimization method for the IR imaging system parameters, on the basis of the modification of λF/d by MRTD model, taking MRTD as the objective function and MTF and NETD as constraints, trading-off MTF and NETD, an automatic optimization method is proposed. This approach can reduce the SWaP$ of the IR imaging system, and provide the theoretical guidance for the development of the IR imaging system. Firstly, considering the relationship between system parameters and the objective function, this section determines the system parameters that needed to be optimized. Then, according to the analysis results, we propose the inverse automatic optimization approach for the IR imaging system parameters.

A. TRADING-OFF AMONG IR SYSTEM PARAMETERS

In the optimization process of the IR imaging system parameters, the main optimization modules in this paper are the

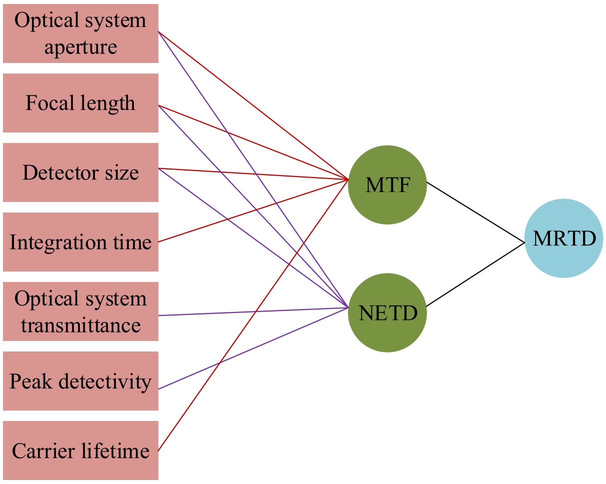

FIGURE 8. The effect of the system parameters on constraints and the objective function.

optical system and the detector. The main system parameters act on the above constraints, further affecting the objective function value. Fig. 8 shows the diagram of the influence of the main system parameters on constraints and the objective function.

According to Fig. 8, when analyzing the influence of system parameters on MRTD, system parameters are constrained by MTF and NETD. The optical system aperture, the focal length, and the detector size are simultaneously constrained by MTF and NETD. The integration time, the optical system transmittance, the peak detectivity, and the carrier lifetime are only constrained by one constraint.

MRTD of the IR imaging system can be satisfied by changing MTF and NETD. Meanwhile, since MRTD is a comprehensive performance, the individual requirement of MTF and NETD should be considered while meeting MRTD requirement. Therefore, when optimizing the IR imaging system parameters, it is necessary to analyze the relationship of each system parameter on different system performance parameters, so that the system can not only meet MRTD requirement, but also avoiding some poor performance, which does not meet the requirement. In this paper, by analyzing the influence trends of each system parameter on performance parameters, the system parameters for the trade-off optimization are obtained. The analysis results of each system parameter on performance parameters are shown in Table 1.

In order to satisfy the design requirement, system parameters need to meet both the objective function and constraints. It can be seen from Table 1 that, monotonic changes in the optical system aperture, the focal length and the detector size, MRTD shows a trend of first increased and then decreased, so the trade-off optimization is required. The other system parameters have monotonic effects on the objective function and constraints, so they are not optimized in this paper. The optical system aperture, the focal length and the detector size determine the value of λF/d. Therefore, the optimization method can be proposed on the basis of the modification of λF/d by MRTD model.

TABLE 1. Optimization parameters.

Parameter	MTF	NETD	MRTD
Optical system aperture↑	Decrease after increase	Decrease	Decrease after increase
Focal length↑	Decrease after increase	Increase	Decrease after increase
Detector size↑	Decrease after increase	Decrease	Decrease after increase
Integration time↑	Increase	-	Decrease
Optical system transmittance↑	-	Increase	Increase
Peak detectivity↑	-	Increase	Increase
Carrier lifetime↑	Decrease	-	Increase

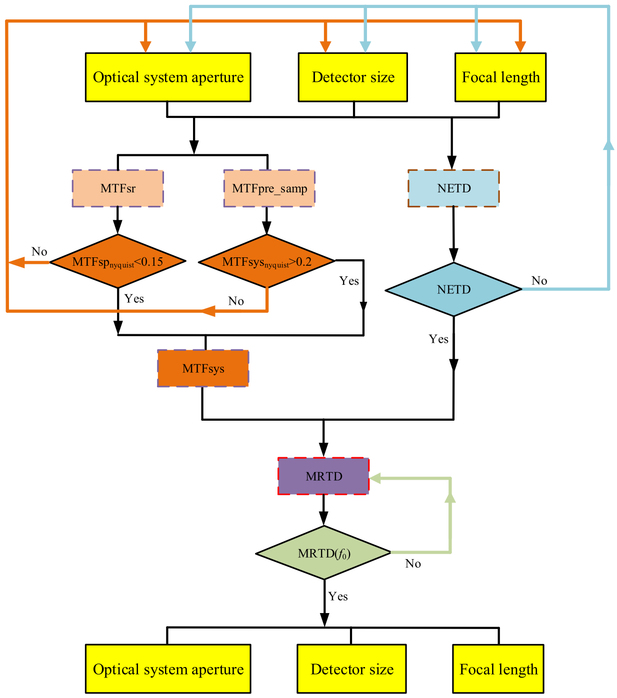

FIGURE 9. Flow chart of optimization method.

B. TRADE-OFF OPTIMIZATION APPROACH FOR IR SYSTEM PARAMETERS

According to the above analysis results, this paper focuses on evaluating the IR imaging system MRTD, combining multiple constraints (MTF and NETD), and simultaneously optimizing the system parameters (optical system aperture, focal length, and detector size), to obtain the optimum parameters of the IR imaging system. The specific optimization method is shown in Fig. 9.

On the basis of the optimization flow chart in Fig. 9, it can be seen that the input parameters are the ranges of the optical system aperture, the focal length and the detector size, and the output parameters are the optical system aperture, the focal length and the detector size that meet the design requirement. First of all, according to the spatial resolution model, by considering the trade-off between the spatial transfer MTF and the spurious response MTF, the parameters that satisfy both the spatial transfer MTF greater than 0.2 and the spurious response MTF less than 0.15 at the Nyquist frequency are selected. Secondly, based on NETD model, the parameters that meet NETD constraint are selected. Finally, for the parameters that meet both MTF and NETD, considering the trade-off between MTF and NETD, the parameters that satisfying MRTD model are selected as optimum parameters. The iterative method is used to optimize the system parameters in this optimization process.

IV. TRADE-OFF OPTIMIZATION RESULTS AND VERIFICATION

In order to verify the rationality of the trade-off optimization method for IR imaging system parameters, the performance requirement is first deduced according to the design requirement. Then, based on the above optimization approach, system parameters (optical system aperture, focal length, and detector size) are optimized simultaneously. Finally, the rationality of the optimization method is verified by comparing the optimization results and the original system.

The design requirement in this paper: CA-295 is optimized to reduce the SWaP$ of the IR imaging system, and at the same time, the imaging performance of the target of 4.00m×4.00m (inherent temperature difference of 3.00K) at 10.00km does not decrease.

Using the MODTRAN software, under the condition of the visibility 20 km, the observer height 0 km, the range 10 km, and in slant path, the average atmospheric transmittance is 0.48. Combining with the inherent temperature difference between the target and the background, the apparent temperature difference at the system aperture can be calculated by (6).

$$\Delta T_{apperent} = \Delta T_{inherent} \times \tau = 3.00K \times 0.48 = 1.44K \quad (6)$$

On the basis of the modified MRTD model, the MRTD curve of CA-295 is shown in Fig. 10.

It can be seen from Fig. 10 that the spatial frequency is 15.00 cyc/mrad when MRTD value is 1.44K. The resolvable cycles on the target can be expressed as:

$$N = f \times \frac{\sqrt{A}}{R} = 15.00cyc/mrad \times \frac{\sqrt{4.00 \times 4.00m}}{10.00km} = 6 \quad (7)$$

According to Johnson criterion, the recognition probability is 80% when the resolvable cycles are 6. In other words, the design requirement is that the recognition probability of the target of 4.00m×4.00m (inherent temperature difference of 3.00K) at 10.00km before and after optimization is 80%. The system parameters of CA-295 are shown in the Table 2.

In the optimization process, it is necessary to ensure that FOV remains unchanged. In order to reduce the complexity of optimization results verification, the selection of the detector in this paper is consistent with CA-295, and the F-number of the optical system is optimized to make the optical system and the detector achieve optimum coupling matching. That is to say, the optimization objective of this paper is that, under the condition that the detector selection remains constant, F-number of the optical system is to be optimized, so that F-number of CA-295 can be optimized to a larger F-number while MRTD value remains unchanged, and the system size becomes smaller.

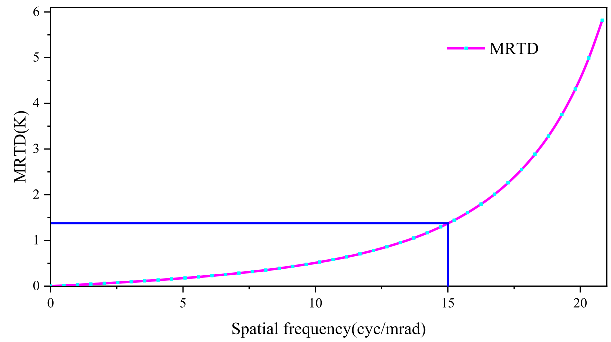

FIGURE 10. MRTD curve of CA-295.

TABLE 2. Parameters of CA-295.

Symbol	Parameter	Value
D	Optical system aperture	317.5mm
EFL	Focal length	1270mm
d	Detector size	25μm

In general, the system is designed for the target and background under the high contrast, so the reduction of the sensitivity in a small range has little effect on the image quality. In the process of the optimization design in this paper, MRTD is guaranteed by increasing the spatial resolution and reducing the sensitivity. According to the analysis of the optimization objective, the objective function is that MRTD at the angular space frequency of 15.00 cyc/mrad is 1.44 K. and the constraints are as follows: the spatial transfer MTF at the Nyquist frequency is not less than 0.2, the spurious response MTF at the Nyquist frequency is not more than 0.15, and NETD is not more than 25 mK.

A. ANALYSIS OF OPTIMIZATION RESULTS

In this paper, the system parameters can be optimized simultaneously. The specific optimization parameters are the optical system aperture, the focal length, and the detector size. In order to reduce the complexity of optimization results verification, the detector size is 25μm, and the focal length is 1270mm according to the FOV. In order to optimize the optical system with a larger F number, λF/d should be greater than λF/d of CA-295 (0.64). Therefore, λF/d range is 0.7∼1.2. The optimization range of the system parameters is shown in Table 3.

Based on the trade-off optimization method for IR system parameters proposed in this paper, the optical system aperture is optimized automatically. Firstly, the trade-off between the spatial transfer MTF and the spurious response MTF is considered, and the optical system aperture range meeting MTF constraint is selected. When λF/d value is 0.7, 0.8 0.9, 1.0, 1.1, and 1.2, respectively, the spatial transfer MTF curve,

TABLE 3. The optimization range of each system parameter.

Symbol	Parameter	Value
EFL	Focal length	1270mm
d	Detector size	25μm
λF/d	λF/d	0.7 to 1.2
F	F-number	4.38 to 7.50
D	Optical system aperture	169.3mm to 290.0mm

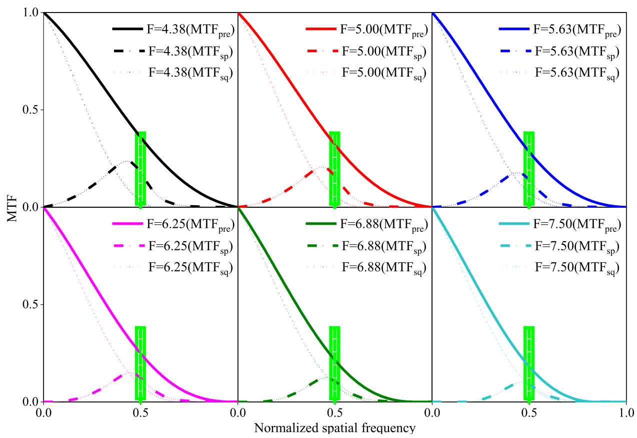

FIGURE 11. MTF curves.

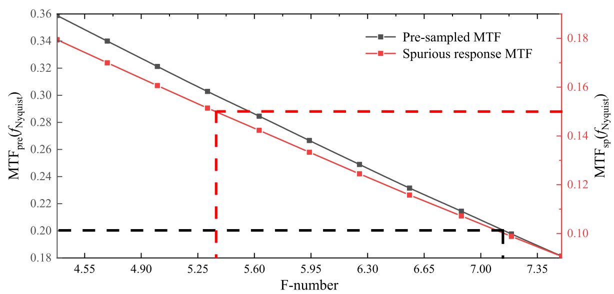

FIGURE 12. MTF value at the Nyquist frequency.

the spurious response MTF curve, and the system MTF curve are shown in Fig. 11. The green dotted line is corresponding to the Nyquist frequency, and the spatial transfer MTF value, the spurious response MTF value, and the system MTF value at the Nyquist frequency are included in the green box.

It can be seen from Fig. 11 that when λF/d value is 0.7 to 1.2, that is, F-number is 4.38 to 7.50, the spatial transfer MTF and the spurious response MTF decreases simultaneously, and the cut-off frequency of each system decreases after spatial sampling. However, the system MTF value first increases and then decreases when the normalized spatial frequency is 0.5. Fig. 12 shows the system MTF curve and the spurious response MTF curve at the Nyquist frequency when the F-number is 4.38 to 7.50.

According to Fig. 12, when F-number is less than 5.38, the system MTF value at the Nyquist frequency is greater than 0.2, but the spurious response MTF value is greater than 0.15. The influence of signal aliasing on the spatial resolution cannot be ignored, which leads to the decrease of the spatial resolution. When F-number is greater than 7.13, the system MTF at the Nyquist frequency is less than 0.2 and the spatial resolution is low. In order to satisfy MTF constraint, F-number should be trading-off. The system parameters satisfying MTF constraint are shown in Table 4. The accuracy of F-number in this paper is 0.01.

TABLE 4. Parameters satisfying the MTF.

λF/d	F	D/mm	MTF_{pre}	MTF_{sp}
0.86	5.38	236.3	0.30	0.15
0.88	5.50	230.9	0.29	0.15
0.90	5.63	225.8	0.28	0.14
0.92	5.75	220.9	0.28	0.14
0.94	5.89	216.2	0.27	0.14
0.96	6.00	211.7	0.26	0.13
0.98	6.13	207.3	0.26	0.13
1.00	6.25	203.2	0.25	0.12
1.02	6.38	199.2	0.24	0.12
1.04	6.50	195.4	0.24	0.12
1.06	6.63	191.7	0.23	0.11
1.08	6.75	188.1	0.22	0.11
1.10	6.88	184.7	0.21	0.11
1.12	7.00	181.4	0.21	0.10
1.14	7.13	178.2	0.20	0.10

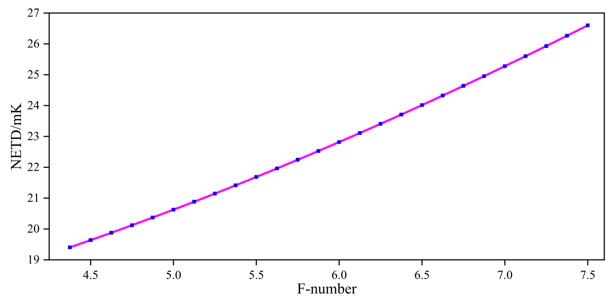

FIGURE 13. NETD value with different F-numbers.

Based on the trade-off between the spatial transfer MTF and the spurious response MTF, it can be seen from Table 4 that when the detector size is 25μm and the focal length is 1270mm, the range of F-number to meet the MTF constraint is 5.38 to 7.13, and the range of the optical system aperture is 178.2mm to 236.3mm.

NETD under different F-numbers are calculated, and the optical system aperture range that meet NETD constraint is selected. Fig. 13 shows NETD curve when the range of F-number is 4.38∼7.25.

It can be seen from Fig. 13 that with the increase of F-number, NETD monotonically increases. Therefore, in order to satisfy NETD constraint, F-number should be as small as possible. When NETD is required to be less than 25mK, the range of F-number is 4.38∼6.88, and the range of optical system aperture is 184.7mm∼290.3mm.

Considering the trade-off between the parameters satisfying MTF constraint in Table 4 and the parameters satisfying NETD constraint, the system parameters satisfying both MTF and NETD are selected as a compromise, as shown in Table 5. The range of F-number is 5.38∼6.88, and the range of optical system aperture is 184.7mm∼236.6mm.

TABLE 5. Parameters satisfying both the MTF and the NETD.

λF/d	F	D/mm	MTF_{pre}	MTF_{sp}	NETD/mK
0.86	5.38	236.3	0.30	0.15	21.41
0.88	5.50	230.9	0.29	0.15	21.69
0.90	5.63	225.8	0.28	0.14	21.96
0.92	5.75	220.9	0.28	0.14	22.24
0.94	5.89	216.2	0.27	0.14	22.53
0.96	6.00	211.7	0.26	0.13	22.82
0.98	6.13	207.3	0.26	0.13	23.11
1.00	6.25	203.2	0.25	0.12	23.41
1.02	6.38	199.2	0.24	0.12	23.71
1.04	6.50	195.4	0.24	0.12	24.01
1.06	6.63	191.7	0.23	0.11	24.32
1.08	6.75	188.1	0.22	0.11	24.64
1.10	6.88	184.7	0.21	0.11	24.95

TABLE 6. Optimum system parameters.

F	D/mm	MTF_{pre}	MTF_{sp}	NETD/mK	MRTD/K
6.50	195.4	0.24	0.12	24.01	1.44

TABLE 7. Optimization results of CA-295.

Parameter	Unit	CA-295	Optimization result
Focal length	mm	1270	1270
Detector size	μm	25	25
F-number	-	4.00	6.50
λF/d	-	0.64	1.04
Optical system aperture	mm	317.5	195.4

For the parameters satisfying both MTF and NETD, MRTD value is calculated to evaluate whether the IR system can satisfy the design requirement. The design requirement of this paper is that when the angular frequency is 15.00 cyc/mrad, the MRTD value is 1.44 K. The system parameters satisfying the MRTD are shown in Table 6. F-number is 6.50, and the optical system aperture is 195.4mm.

On the basis of the optimization method proposed in this paper, for the target with a recognition probability of 80%, the optimization results of CA-295 are shown in Table 7.

B. VERIFICATION

In order to verify the rationality of the optimization approach proposed in this paper, combining the above optimization results, the performance parameters and image simulation of CA-295 before and after optimization are compared in this section.

1) PERFORMANCE PARAMETERS VERIFICATION

In order to visually compare the system performance before and after optimization, Table 8 shows the performance parameters of CA-295 before and after optimization.

It can be seen from Table 8: (1) FOV and MRTD of the system before and after optimization remain the same, which indicates the same comprehensive performance, and

TABLE 8. Performance parameters of CA-295 before optimization and after optimization.

Parameter	Unit	CA-295	Optimization result
MRTD(f=15.00cyc/mrad)	K	1.44	1.44
FOV	mrad	40.96	40.96
λF/d	-	0.64	1.04
$MTF_{sys}(f_{Nyquist})$	-	0.38	0.24
$MTF_{sr}(f_{Nyquist})$	-	0.19	0.12
NETD	mK	18.73	24.01

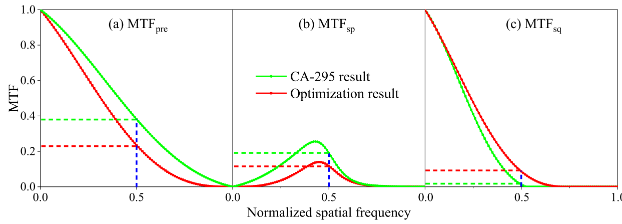

FIGURE 14. MTF curves of CA-295 before and after optimization.

the design requirement is satisfied. (2) λF/d increases from 0.64 to 1.04, that is, F-number of the optical system increases from 4.00 to 6.50. The increase of F-number reduces the SWaP$ of the IR imaging system. (3) At the Nyquist frequency, the system MTF value decreases from 0.38 to 0.24, and the spurious response MTF value reduces from 0.19 to 0.12, which improves the spatial resolution and satisfies MTF constraint. (4) NETD increases as the spatial resolution increases, that is, the sensitivity decreases. However, NETD is still less than 25mK, which meets the design requirement.

Based on the optimization results of Table 7, Fig. 14 and Fig. 15 more clearly analyze the difference between MTF and MRTD before and after optimization. Fig. 14 and Fig. 15 respectively describe MTF curves and MRTD curves of CA-295 before and after optimization. Among them, the green curve represents the performance curve of CA-295, and the red curve shows the performance curve after optimization,

Fig. 14(a) shows the spatial transfer MTF curve, in which the spatial transfer MTF value at the Nyquist frequency before and after optimization is 0.38 and 0.24, respectively. Fig. 14(b) shows the spurious response MTF curve, where the spurious response MTF value at the Nyquist frequency before and after optimization is 0.19 and 0.12, respectively. Fig. 14(c) shows the system MTF curve after considering the trade-off between the spatial transfer MTF and the spurious response MTF. The system MTF value at the normalized spatial frequency of 0.5 is 0.01 and 0.08, respectively. That is to say, trading-off the spatial transfer MTF and the spurious response MTF, the spatial resolution after optimization is higher than that of CA-295.

Fig. 15 shows MRTD curve of CA-295 before and after optimization. The intersection of the two blue lines indicate that when the angular space frequency is 15.00cyc/mrad, MRTD value is 1.44 K.

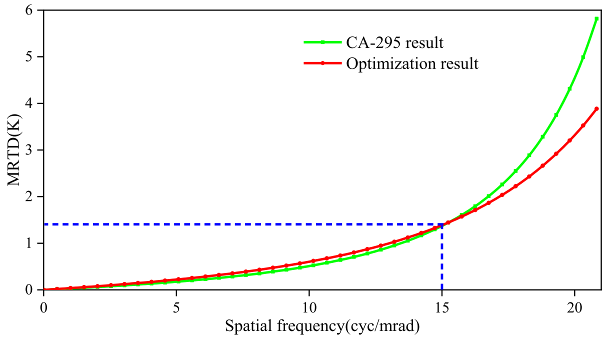

FIGURE 15. MRTD curves of CA-295 before and after optimization.

According to Fig. 15, it can be seen that when the angular spatial frequency is less than 15.00 cyc/mrad, MRTD value of CA-295 is smaller than that after optimization, and when the angular space frequency is more than 15.00 cyc/mrad, MRTD value of CA-295 is larger than that after optimization. Therefore, the optimization method proposed in this paper is only suitable for the condition where the contrast is not lower than the design requirement. That is to say, for the optimization objective in this paper, the optimization result can only ensure that when the spatial frequency is not less than 15.00cyc/mrad, the performance of the system after optimization will not decrease compared to CA-295.

2) SIMULATION VERIFICATION

In this section, two-dimensional image simulation is used to verify the rationality of the optimization method. The physical size of the first-bar test target is 10.60m×1.51m, the inherent temperature difference between the target and the background is 3.00K, the wavelength range is 3μm to 5μm, and the imaging distance is 6km, 10km, and 12km respectively. When the imaging distance is 10km and the recognition probability is 80%, the spatial frequency of the first-bar test target is 15.00cyc/mrad, which is the same as the design requirement in this paper.

Evaluating the simulated images in Fig. 16 through human eye observation shows that when the imaging distance is 10km, the imaging results of the four-bar test target are the same before and after the optimization, which means the simulation results satisfying the design requirement. When the imaging distance is 8 km, due to the decrease of the atmospheric attenuation, the apparent temperature difference at the system aperture increases. The system after optimization corresponds to a larger spatial frequency when the temperature difference is large, that is to say, the resolvable cycles on the target is more. Therefore, the recognition probability of the system after optimization is greater than that of CA-295. When the imaging distance is 12 km, the atmospheric attenuation increases, so the apparent temperature difference at the system aperture decreases. CA-295 corresponds to a larger spatial frequency when the temperature difference is small, that is, the resolvable cycles on the target is more. As a result, the recognition probability of CA-295 is greater than that of the system after optimization. All in all, the optimized results in this paper are suitable for high-contrast target imaging.

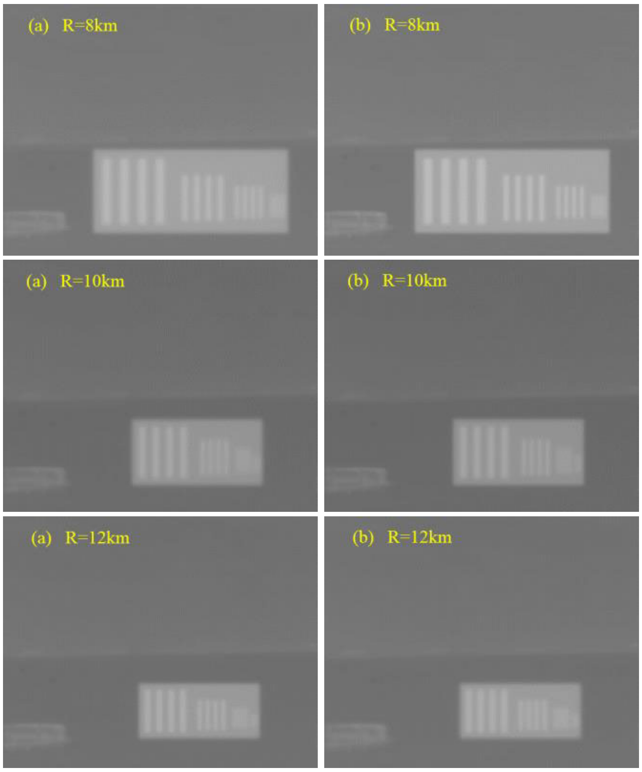

FIGURE 16. Simulation results. (a) Simulation results of CA-295. (b) Simulation results of the system after optimization.

Through the above simulation results and analysis, the optimization results in this paper can satisfy the design requirements, and the imaging performance of the system after optimization is better than CA-295 under high contrast conditions.

V. CONCLUSION

Considering the trade-off between the spatial resolution and the sensitivity, this paper modifies λF/d by MRTD model, and proposes a general trade-off optimization approach, which can simultaneously optimize the main system parameters, such as the optical system aperture, the focal length, and the detector size. For the system parameters of given ranges, we can automatically select the optimum IR imaging system parameters, which can reduce the SWaP$ of the IR imaging system. The rationality of the proposed optimization method is verified by optimizing the system parameters of CA-295. The research work in this paper provides the data support for design and optimization of the IR imaging system.

REFERENCES

[1] K. Zhang, K. Yang, S. Li, and H.-B. Chen, "A difference-based local contrast method for infrared small target detection under complex background," *IEEE Access*, vol. 7, pp. 105503–105513, 2019, doi: 10.1109/ACCESS.2019.2932729.

[2] S. Ma, Z. Tao, X. Yang, Y. Yu, X. Zhou, and Z. Li, "Bathymetry retrieval from hyperspectral remote sensing data in optical-shallow water," *IEEE Trans. Geosci. Remote Sens.*, vol. 52, no. 2, pp. 1205–1212, Feb. 2014.

[3] S. J. Krotosky and M. M. Trivedi, "Person surveillance using visual and infrared imagery," *IEEE Trans. Circuits Syst. Video Technol.*, vol. 18, no. 8, pp. 1096–1105, Aug. 2008.

[4] C. Gaudin-Delrieu, J. L. Lamard, P. Cheroutre, B. Bailly, P. Dhuicq, and O. Puig, "The high resolution optical instruments for the Pleiades HR Earth observation satellites," in *Proc. 7th Int. Conf. Space Opt. (ICSO)*, 2008, pp. 14–17.

[5] M. Tristan Goss and J. Cornelius Willers, "Small pixel cross-talk MTF and its impact on MWIR sensor performance," *Proc. SPIE*, vol. 10178, May 2017, Art. no. 101780L.

[6] A. N. Enemuo, R. R. Chaudhuri, Y. Song, and S.-W. Seo, "Thermo-optic sensor based on resonance waveguide grating for Infrared/Thermal imaging," *IEEE Sensors J.*, vol. 15, no. 8, pp. 4213–4217, Aug. 2015.

[7] R. G. Driggers, "Infrared detector size: How low should you go?" *Opt. Eng.*, vol. 51, no. 6, Jun. 2012, Art. no. 063202.

[8] D. Knežević, A. Redjimi, K. Knežević, D. Vasiljević, Z. Nikolić, and J. Babić, "Minimum resolvable temperature difference model, simulation, measurement and analysis," *Opt. Quantum Electron.*, vol. 48, no. 6, p. 332, Jun. 2016.

[9] G. C. Holst and R. G. Driggers, "Small detectors in IR system design," *Opt. Eng.*, vol. 51, no. 9, Sep. 2012, Art. no. 096401.

[10] P. Bijl and M. A. Hogervorst, "EO system design and performance optimization by image-based end-to-end modeling," *Proc. SPIE*, vol. 11001, May 2019, Art. no. 110010G.

[11] C. Olson, M. Theisen, T. Pace, C. Halford, and R. Driggers, "Model development and system performance optimization for staring infrared search and track (IRST) sensors," *Proc. SPIE*, vol. 9820, May 2016, Art. no. 98200B.

[12] G. C. Holst, "Is there an optimum detector size for digital night vision goggles?" *Proc. SPIE*, vol. 9820, May 2016, Art. no. 98200C.

[13] C. Liu, J. Lin, and M. Tseng, "Design of CMOS sensor fill factor for optimal MTF and SNR," *Proc. SPIE*, vol. 7826, no. 2, Oct. 2010, Art. no. 78261N.

[14] M. Abolghasemi and D. Abbasi-Moghadam, "Design and performance evaluation of the imaging payload for a remote sensing satellite," *Opt. Laser Technol.*, vol. 44, no. 8, pp. 2418–2426, 2012.

[15] X. Xiao, F. Pan, W. Li, Q. Gao, and D. Xiong, "The objective measurement method of minimum resolvable temperature difference for infrared imaging system based on ANFIS," in *Proc. IEEE Int. Conf. Fuzzy Syst. (FUZZ-IEEE)*, Vancouver, BC, Canada, Jul. 2016, pp. 837–843, doi: 10.1109/FUZZ-IEEE.2016.7737775.

[16] Z. Liu, H. Mao, Y. Dai, and J. Wu, "A new infrared sensor model based on imaging system test parameter," in *Proc. IEEE Int. Conf. Green Comput. Commun. IEEE Internet Things IEEE Cyber, Phys. Social Comput.*, Beijing, China, Aug. 2013, pp. 1953–1956, doi: 10.1109/GreenCom-iThings-CPSCom.2013.364.

[17] S. D. Gunapala, "Modulation transfer function of infrared focal plane arrays," in *Proc. IEEE Photon. Conf.*, Bellevue, WA, USA, Sep. 2013, pp. 600–601, doi: 10.1109/IPCon.2013.6656437.

[18] S. D. Gunapala, D. Z. Ting, J. Nguyen, A. Soibel, S. B. Rafol, A. Khoshakhlagh, J. M. Mumolo, J. K. Liu, S. A. Keo, and A. Liao, "Pixel-to-pixel cross-talk of infrared focal plane arrays," in *Proc. IEEE Photon. Conf.*, Burlingame, CA, USA, Sep. 2012, pp. 232–233, doi: 10.1109/IPCon.2012.6358577.

[19] D. P. Haefner, J. Stevens, M. Groenert, S. Burks, M. Dnyder, and C. Dumn, "Post-optic MTF measurement using a reference optic," *Proc. SPIE*, vol. 10625, Apr. 2018, Art. no. 106250B.

[20] J. Schuster, "Numerical simulation of the modulation transfer function (MTF) in infrared focal plane arrays: Simulation methodology and MTF optimization," *Proc. SPIE*, vol. 10526, Art. no. 105261I, Feb. 2018.

[21] B. Appleton, T. Hubbard, A. Glasmann, and E. Bellotti, "Parametric numerical study of the modulation transfer function in small-pitch InGaAs/InP infrared arrays with refractive microlenses," *Opt. Exp.*, vol. 26, no. 5, pp. 5310–5326, 2018.

[22] H. Yang, Y. Wang, and T. T. Tschudi, "Optimization of sampled imaging system with baseband response squeeze model," *Proc. SPIE*, vol. 6834, Nov. 2007, Art. no. 683419.

KE LI received the B.E. degree in optoelectronic information engineering from Xi'an Technological University, China, in 2015. She is currently pursuing the Ph.D. degree in optical engineering with the School of Physics and Optoelectronic Engineering, Xidian University. Her research interests include modeling, design, and optimization of infrared imaging systems.

YING YUAN received the B.E. degree in electronic science and technology and the Ph.D. degree in optical engineering from Xidian University, China, in 2011 and 2018, respectively. From 2018 to 2020, she was a Postdoctoral Fellow with Xidian University. Her research interests include integral imaging 3D display, light field of imaging, and infrared technology. She is a member of the Optical Society of China.

CHAO ZHANG received the B.E. degree in optoelectronic information science and engineering from Xidian University, China, in 2017, where he is currently pursuing the Ph.D. degree in optical engineering with the School of Physics and Optoelectronic Engineering. His research interests include the simulation and evaluation of optoelectronic countermeasures.

HANG YUAN received the B.E. degree in measurement-control technology and instrumentation specialty from Xi'an Technological University, China, in 2015. She is currently pursuing the Ph.D. degree in optical engineering with the School of Physics and Optoelectronic Engineering, Xidian University. Her research interests include simulation, experiment, and evaluation of infrared multispectral imaging of air-space targets.

XIAORUI WANG received the B.S. degree in optoelectronics technology from Sichuan University, China, in 1998, and the Ph.D. degree in optical engineering from the School of Physics and Optoelectronic Engineering, Xidian University, China, in 2005. From 2007 to 2008, as a Visiting Scholar, he conducted scientific cooperative research in the 3DVIS Laboratory, Optical Center, The University of Arizona, USA. In 2010, he was promoted to a Professor exceptionally. His research interests include advanced optical remote sensing photogrammetry and photoelectric simulation, three-dimensional imaging display, virtual reality and augmented reality, and micro-nano optics and integrated optical information processing.